



ELSEVIER

Journal of Chromatography A, 703 (1995) 503–522

JOURNAL OF
CHROMATOGRAPHY A

Performance characteristics of a real-time direct deposition supercritical fluid chromatography–Fourier transform infrared spectrophotometry system

Kelly L. Norton¹, Peter R. Griffiths*

Department of Chemistry, University of Idaho, Moscow, ID 83844-2343, USA

Abstract

In this paper, real-time, on-line measurements of direct deposition capillary supercritical fluid chromatography–Fourier transform infrared spectra of subnanogram quantities of analytes is demonstrated for the first time. The minimum identifiable quantity for caffeine (a strong infrared absorber) obtained with this interface was 600 pg (injected) and 1–10 ng for weaker absorbers. Spectra over the entire mid-infrared region of compounds separated with a mobile phase of carbon dioxide modified with two percent methanol were able to be measured. The interface shows linear behavior over two orders of magnitude for both the area under a strong absorption band in the infrared spectra versus injected quantity and for the area under a peak from the functional group chromatogram versus injected quantity.

1. Introduction

Two distinct approaches for interfacing chromatographs and Fourier transform infrared (FTIR) spectrophotometers have been described. In the first and most commonly utilized interface, the infrared spectra of the effluent from a chromatographic column are measured continuously as the effluent passes through a flow-cell. In the second approach, the infrared spectra of the eluents are measured after they are deposited on a suitable substrate. In general, the flow-cell technique is instrumentally simple but

has the disadvantage of low sensitivity. Both approaches have been implemented for supercritical fluid chromatography (SFC) coupled with FTIR with the direct deposition (DD) measurements having been made both in the off-line [1–7] and on-line [8,9] mode. In this paper, the first on-line DD SFC–FTIR spectrophotometer is described and the performance characteristics are reported.

The use of high-pressure flow-cells in capillary column SFC–FTIR measurements has been implemented by several groups [10–18]. A flow-cell for SFC–FTIR must be able to withstand the high pressures used in SFC and must be constructed using infrared transparent windows. Even though spectra of injected quantities of 10 to 100 ng have been measured using a flow-cell with CO₂ as the mobile phase, this technique

* Corresponding author.

¹ Present address: Abbott Laboratories, North Chicago, IL 60064-4000, USA.

suffers from several disadvantages. The most important disadvantage is the loss of part of the infrared spectrum due to absorption by the mobile phase, unless the CO₂ mobile phase is replaced by xenon [7,11,16–18]. The fraction of the spectrum lost is determined by the absorption properties of the mobile phase. The most common mobile phase for SFC is carbon dioxide, the spectrum of which exhibits several absorption bands including three that are totally absorbing under SFC–FTIR conditions [10,11,15]. The use of pressure ramps in SFC–FTIR exacerbates the problem by making subtraction of the background absorption due to CO₂ more difficult. Also, the addition of polar modifiers to the mobile phase to decrease the retention time of polar compounds, in particular for packed-column SFC, obscures an even larger portion of the infrared spectrum. One way to circumvent the effect of excessive absorption from the mobile phase is to limit the pathlength of the flow-cell; this approach, however, further reduces the sensitivity in the spectral windows.

Another disadvantage in using flow-cells for SFC–FTIR measurements is the difficulty in performing spectral searching. Even if the spectrum can be measured with a high signal-to-noise ratio (S/N), the position of the absorption bands of the solutes varies with the temperature and pressure of the mobile phase [19]. Thus to obtain useful spectral searching results, the reference spectra should be taken with the same mobile phase at the same temperature and pressure as the corresponding parameters under which the spectrum of the unknown was taken.

Neither of the problems discussed above for flow-cell chromatography–FTIR techniques is encountered when the mobile phase is eliminated before measurement of the infrared spectrum. The elimination of the mobile phase is facilitated in SFC–FTIR since most mobile phases are gaseous at standard temperature and pressure (STP). This approach was first demonstrated by Shafer et al. [1] who deposited the elutes on a moving glass plate on which a layer of powdered KCl had been laid down from a methanol slurry. The plate was then taken to a

FTIR spectrophotometer where diffuse reflectance measurements of the deposited spots were made. Further work by the same group [2–4] and others [5–7] showed that superior results could be obtained by depositing the elutes directly on a moving ZnSe substrate and measuring transmittance spectra under an FTIR microscope. Similar off-line DD interfaces have been developed for gas chromatography (GC)–FTIR [4,20,21] and HPLC–FTIR [22–31] spectrophotometry. On-line GC–FTIR measurements using this approach were reported by us [32,33] and others [34–39].

The key to the high sensitivity in the DD technique is to deposit each elute in a very small area, which leads to an increase in its thickness and, therefore, its absorbance. Pentoney et al. [2,3] demonstrated that the elutes from a capillary SFC column could be deposited on a moving ZnSe window as spots with a diameter of less than 150 μm. Spectra of the analytes then could be measured using an FTIR microscope. A detailed description of why the elutes should be deposited in such a small area to yield the maximum sensitivity was discussed by Griffiths et al. [8]. Elimination of the mobile phase before measurement of the spectra also eliminates the influence of the temperature and pressure of the mobile phase on the spectrum, thereby allowing spectral searching of DD SFC–FTIR data to be accomplished against standard condensed phase libraries [40,41].

In this paper, we demonstrate the detection limits, the minimum identifiable quantity and response linearity obtained with a *real-time* SFC–FTIR interface based on a commercial direct deposition GC–FTIR system. The feasibility of measuring spectra of compounds separated using polar modifiers in the mobile phase is also demonstrated.

2. Experimental

A DD GC–FTIR interface, the Tracer (Diligab Division of Bio-Rad Laboratories, Cambridge, MA, USA) which has been described by

Bourne et al. [33] was slightly modified to obtain SFC–FTIR measurements. In this device, the beam from a Bio-Rad Digilab Model FTS-60 spectrophotometer is focused onto a 60×30 mm ZnSe window by a 5-cm focal-length ellipsoidal mirror. The transmitted beam is collected by a Schwarzschild microscope objective and refocused by a field lens at an adjustable rectangular aperture, which defines the effective size of the infrared beam at the ZnSe window. The beam is refocused by a matched Schwarzschild microscope objective onto a 100×100 μm mercury cadmium telluride detector. The modifications to the Tracer required for SFC–FTIR operation were relatively simple. The 1.5-meter long transfer line, which terminates into an 8-cm long piece of 50- μm internal diameter (I.D.) fused-silica incorporating an orifice/restrictor, was replaced by a 1.5-meter long, 50- μm I.D. transfer line that terminates into an integral restrictor [42] (White Associates, Pittsburgh, PA, USA). The transfer line was maintained at a temperature equal to the temperature of the column. The end of the restrictor for the SFC–FTIR experiments was positioned about 75 μm from the ZnSe window and was heated to 100°C by a cartridge heater. The ZnSe window is cooled to approximately -10°C ($\pm 10^\circ\text{C}$) with a methanol–dry-ice mixture to trap the eluents efficiently without condensing the mobile phase. The optimum speed to translate the deposition window was selected to maintain an appropriate compromise between chromatographic resolution and spectroscopic sensitivity. The best compromise is obtained when the distance moved by the window during the time equal to the full width at half height (fwhh) of the narrowest peak in the chromatogram is equal to the diameter of the spot deposited on a stationary window. The speed at which the ZnSe window was translated was reduced from approximately 1200 $\mu\text{m}/\text{min}$, which had been found to be optimum for DD capillary GC–FTIR measurements, to approximately 100 $\mu\text{m}/\text{min}$. This decrease in speed reflects the increase in the peak width of SFC peaks as compared with GC peaks. Because of this slow speed, there was a time delay of

approximately 3 min from the time an eluate emerges from the column and the time its spectrum was acquired. All spectra shown in this paper were measured in ‘real time’, that is measured as each eluate passes through the infrared beam, and at a resolution of 8 cm^{-1} . The measurement time for the spectra shown in this paper varies from about 0.3 to 2 min.

The 170 l/s turbomolecular pump maintained a pressure below 0.1 mTorr at all SFC pressure conditions (up to an STP CO_2 flow-rate of 5 ml/min). This pumping speed was fast enough that virtually no absorption due to CO_2 was observed.

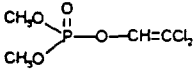
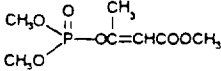
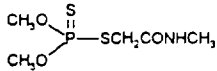
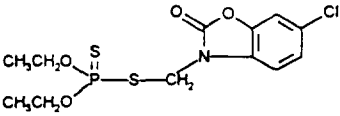
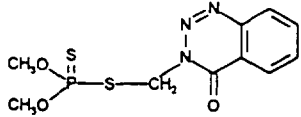
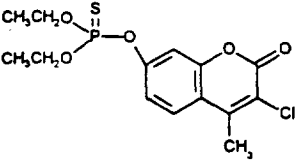
The SFC separations were performed on a 10-m long, 100- μm I.D. 0.25- μm thick SB-Biphenyl-30 capillary column (Lee Scientific, Salt Lake City, UT, USA) installed in a Hewlett-Packard 5890 gas chromatograph. The mobile phase was pumped with a Computer Chemical Systems 7000 SFC Fluid/Controller Delivery System, in the linear pressure program mode. Injections of 60 nl of the sample solutions were accomplished using an air-driven valve (Valco, Houston, TX, USA).

3. Results and discussions

3.1. Chromatographic resolution

An examination of the chromatographic resolution of the system was performed by injecting a mixture of six phosphorus(V) cholinesterase inhibitor pesticides into the system. In Table 1, the elution order, trivial names, trade names and structures of these pesticides are listed. Fig. 1 shows a SFC–FTIR Gram-Schmidt (GS) reconstructed chromatogram [43] and the overlaid chromatograms of the flame ionization detection (FID) traces of the six pesticides. (The pesticides were injected individually to allow the presence of impurities or other components in each sample to be detected.) The difference in the retention times is caused by the installation of different restrictors in the FID and SFC–FTIR interface. Peaks 2a and 2b in the chromatograms

Table 1
Elution order, trivial names (trade names) and structures of six cholinesterase inhibitor pesticides

Elution order	Chemical named (trade name)	Structure
1	Dichlorvos (DDVP)	
2	Mevinphos (Phosdrin)	
3	Dimethoate (Cygon)	
4	Phosalone (Zolone)	
5	Azinphos-methyl (Guthion)	
6	Coumaphos (Col-Ral)	

are from Phosdrin, which contains 40% of other active related compounds. The elutes were deposited as spots with a diameter of approximately 200 μm and not 100 μm as the DD GC-FTIR instrument. It can be seen that there is a difference in resolution between the FID and GS chromatograms mostly because of an increase in the peak widths of the first peaks in the GS chromatogram. The FID trace shows the normal chromatographic behavior of larger peak widths at increased retention times. The SFC-FTIR chromatogram shows virtually no change in the peak widths with retention time. This

suggests the SFC-FTIR peak widths are determined by the deposition and not by the chromatography. If the slight resolution loss is important, then the translation speed of the ZnSe window could be increased, at the cost of a small loss of sensitivity. If, for example, the translation speed is doubled, the thickness of the layer, and hence the spectroscopic sensitivity, is halved. There is, however, no increase in the diameter of the deposited spots (and therefore no further degradation of the chromatographic resolution) with increases in the amount of compound injected. Fig. 2 shows 3-D plots of the

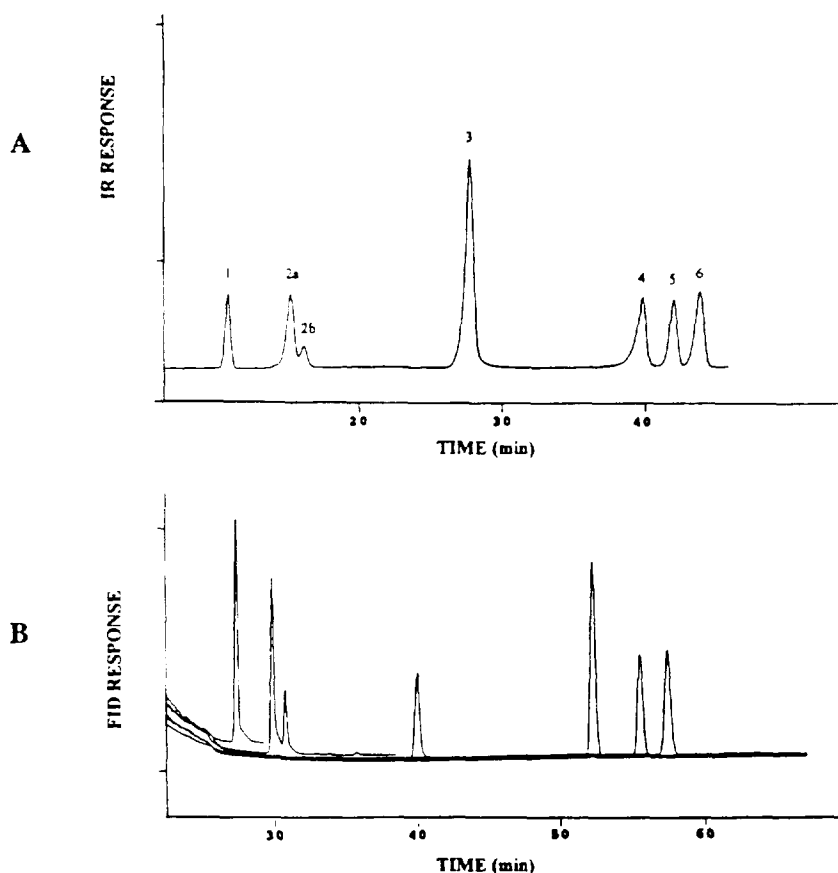


Fig. 1. Chromatograms of six cholinesterase inhibitor pesticides: (A) SFC-FTIR Gram-Schmidt reconstructed chromatogram; (B) FID traces for the six pesticides injected individually.

deposition profiles of different injected amounts of acenaphthenequinone from chromatographic runs (on a moving window). Each slice is the plot of the absorbance at 1720 cm^{-1} from spectra taken in $100\text{-}\mu\text{m}$ increments across the width of the deposited spot. Each slice is also separated by $100\text{ }\mu\text{m}$ along the length of the deposited eluents. As seen in Fig. 2, the deposition profile is the same for injection amounts of 10 ng to at least 120 ng .

3.2. Quantification

The accuracy of quantification by this technique was investigated by injecting mixtures of

acenaphthenequinone and caffeine at varying concentrations. The linearity was checked using the chromatographic peak areas and heights and the areas and heights of the carbonyl stretching bands in the spectra of both compounds. The chromatograms were integrated using LabCalc (Galactic Industries, Salem, NH, USA) and the spectral areas and heights were obtained by curve fitting the regions of interest using the LabCalc curve fitting routine. All data points shown are from the average of three injections. All regression results that will be shown were calculated without using the data from the 300 pg injections (where the S/N is very low), but all graphs will be shown with this point included.

Chromatograms can also be obtained by inte-

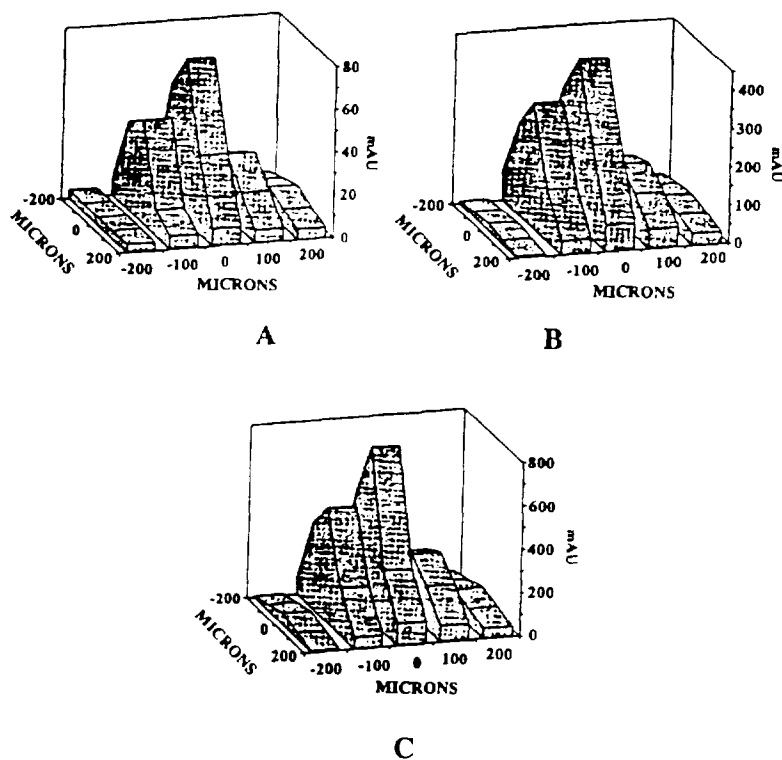


Fig. 2. Depositional profiles of acenaphthenequinone from the DD SFC–FTIR interface: injections of (A) 10 ng; (B) 60 ng; and (C) 120 ng.

grating the absorbance in selected spectral regions, called functional group (FG) chromatograms by the Digilab software. The concentration curves for the FG chromatograms (calculated from the absorbance between 1800–1600 cm^{-1}) using both peak area and height were linear for both compounds tested from at least 600 pg to 60 ng injections. The linear regression results calculated from the FG chromatographic peak area for caffeine from 600 pg to 90 ng gave a correlation coefficient of 0.9995. The regression results for the same range for caffeine using the peak height data gave a correlation coefficient of 0.9989. The corresponding plots for acenaphthenequinone were only linear (correlation coefficient of 0.9996) to 60 ng, above which a negative deviation was observed.

Calculations for linearity were also obtained

on the GS reconstructed chromatograms. Even though fairly high correlation coefficients (>0.999 for peak area and >0.995 for peak height) were obtained for both caffeine and acenaphthenequinone, further inspection showed the curves were not very linear. The calibration plot curve for caffeine (regression line calculated from 600 pg to 90 ng) is shown in Fig. 3A. No data could be obtained for the 300 pg injections for the GS chromatograms because the S/N was below 2. As shown in the expanded plot in Fig. 3A, the points corresponding to injections of less than 2 ng are below the calculated line. This effect is presumably related to the relatively low S/N of these peaks causing baseline errors. The apparently high regression coefficient, even though the points near the origin all fall below the best-fit straight line, is a problem associated

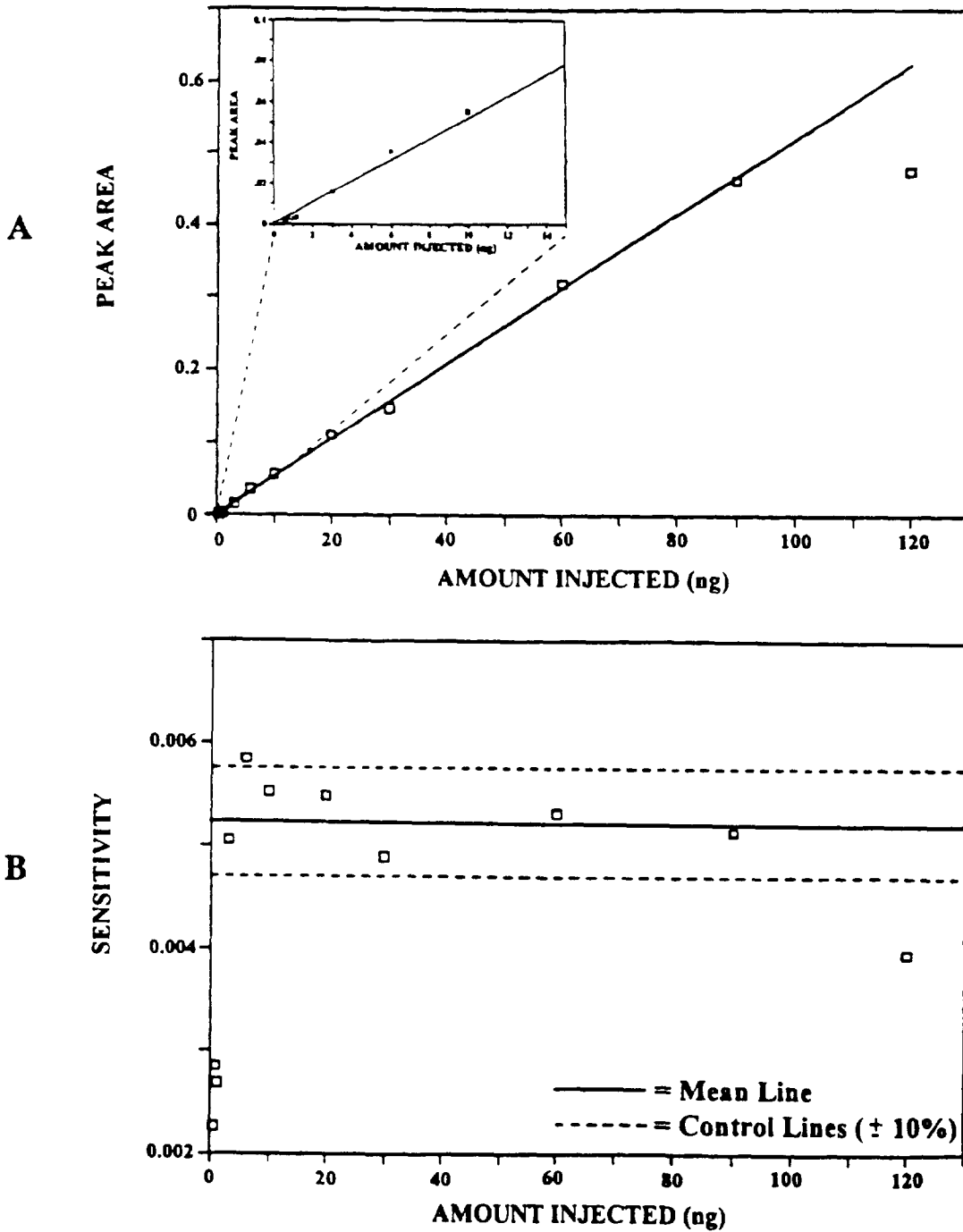


Fig. 3. Calibration curves for caffeine from Gram-Schmidt reconstructed chromatographic data: (A) linear regression plot and (B) linearity plot.

with the use of linear regression calculations over a fairly large range (over 2 orders of magnitude in injected quantity). Although a correlation coefficient of 0.9995 was obtained from these data, the curve is skewed to a smaller slope and a higher y-intercept by the data points corresponding to higher injected amount.

An easier way to observe this problem without expanding the graph is to plot the data as *linearity plots* as described by Cassidy and

Janoski [44] (Fig. 3B). To obtain these linearity plots, the analytical response (peak or absorbance area or height) is divided by the concentration (amount injected) of the standard to give the *sensitivity* for each data point, and the sensitivity is plotted versus the amount injected. Two parallel lines representing the acceptable upper and lower error ranges are also drawn on the plot to determine the linear range. The outer (control) lines for the graphs shown in this paper

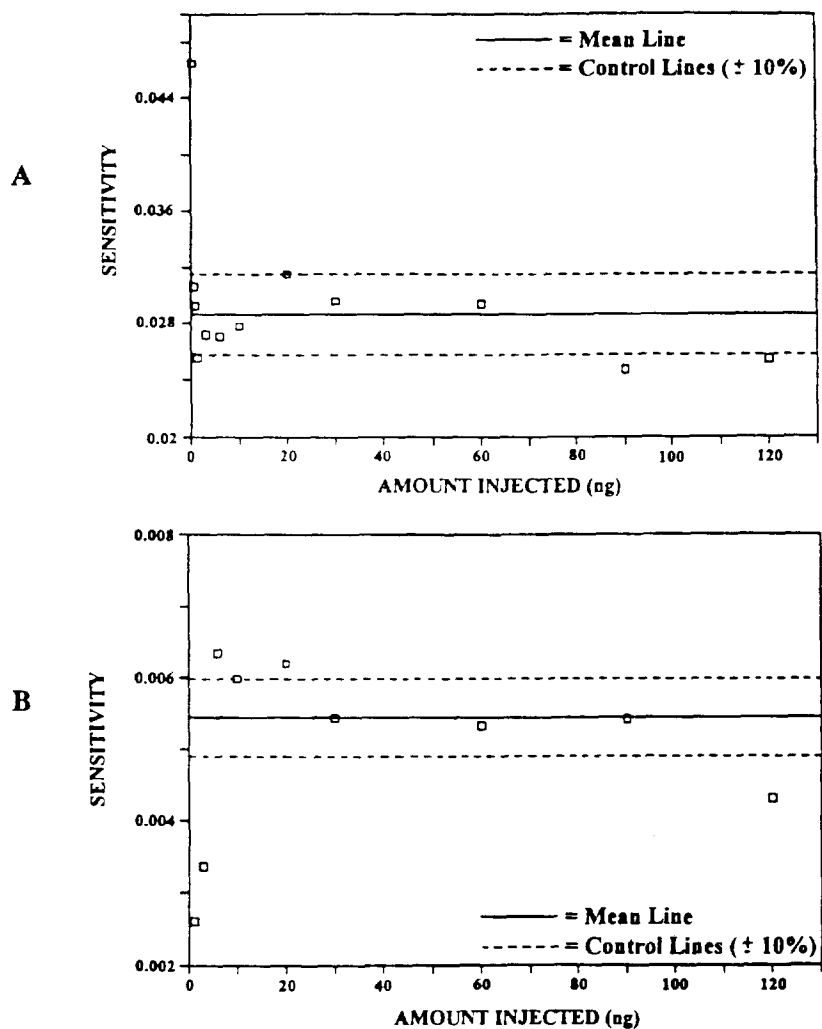


Fig. 4. Linearity plots for acenaphthenequinone from (A) functional group chromatograms and (B) Gram-Schmidt reconstructed chromatograms.

are for an error of 10%. The central (mean) line was determined by averaging only the data points falling inside the control lines. The sensitivity values of all the plots shown have been corrected for any non-zero y-intercept obtained. The data points at the lower limit are especially susceptible to non-zero intercepts distorting the shape of the plot. The y-intercepts were calculated by performing a linear regression analysis on those data points falling on or very near the

regression line (e.g., for Fig. 3B, the 1.2 and 6 ng points were not used). The calculated y-intercept was then subtracted from the analytical response before dividing by the amount injected to give the sensitivity for each data point.

As shown in Fig. 3B, injected quantities of less than 3 ng led to errors of greater than 30% in comparison to the data points for larger injected quantities. The corresponding plots for caffeine using peak height data were similar but were

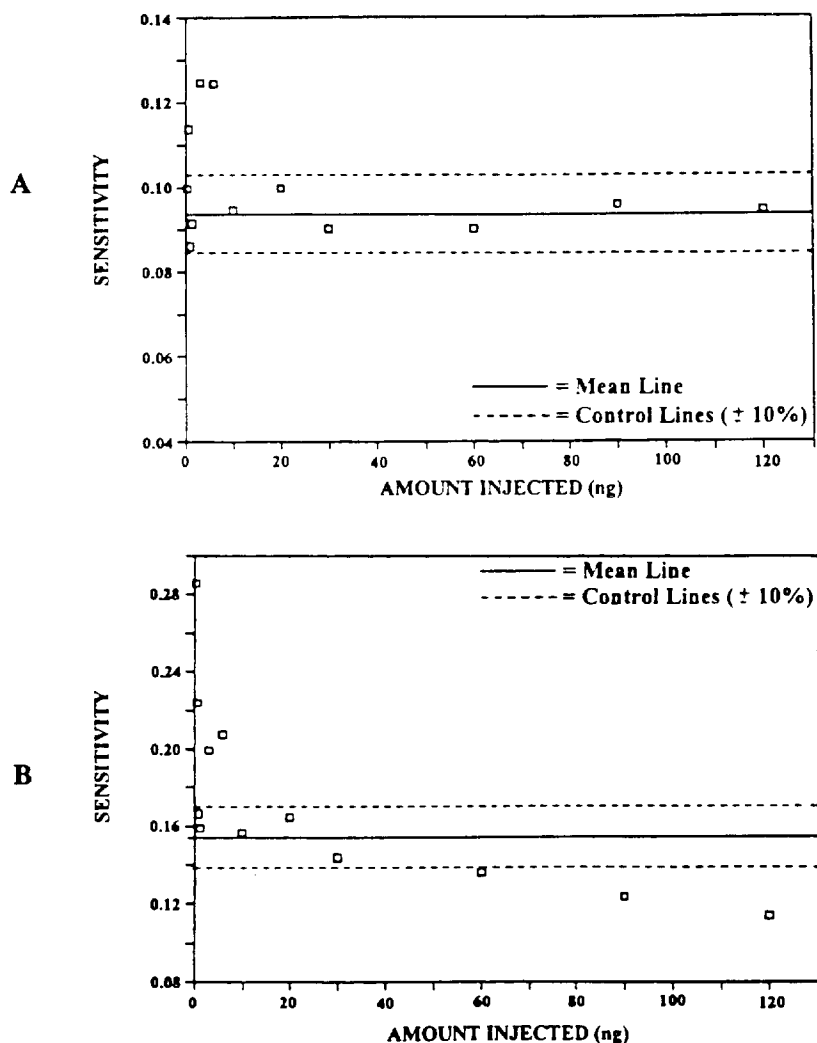


Fig. 5. Linearity plots using IR absorbance area for caffeine: bands at (A) 1700 cm^{-1} and (B) 1660 cm^{-1} .

quantitatively slightly worse. The peaks from injections of less than 1.2 ng of acenaphthenequinone could not be integrated accurately, but all of the chromatograms were expanded and the peak heights were estimated manually. A correlation coefficient of 0.9991 was obtained for the GS peak area data for injected quantities from 1.2 ng to 90 ng. Even though a high correlation coefficient was obtained for the GS peak area data, the plots are not very linear. This can easily be seen in comparing the linearity plots from the FG and GS chromatograms shown in Fig. 4. The peak height data gave a correlation coefficient of only 0.995 and are, therefore, not correlated very well.

From these data, it can be seen that the GS reconstructed chromatograms are not useful for

estimating the quantity of a given component over a wide range as they are only linear over approximately 1 order of magnitude. Not unexpectedly, these chromatograms are more adversely affected by baseline shifts and small levels of contaminants on the window than the FG chromatograms. The low S/N with the low levels of sample injected also contribute to the lack of linearity. The use of functional group chromatograms (which have a higher S/N, especially for compounds with strong absorption bands) affords a good way of approximating the injected quantity of a component within $\pm 15\%$ over 2 orders of magnitude.

The variation of the absorbance of the carbonyl stretching bands in the spectra of the two probe molecules was also used to examine the

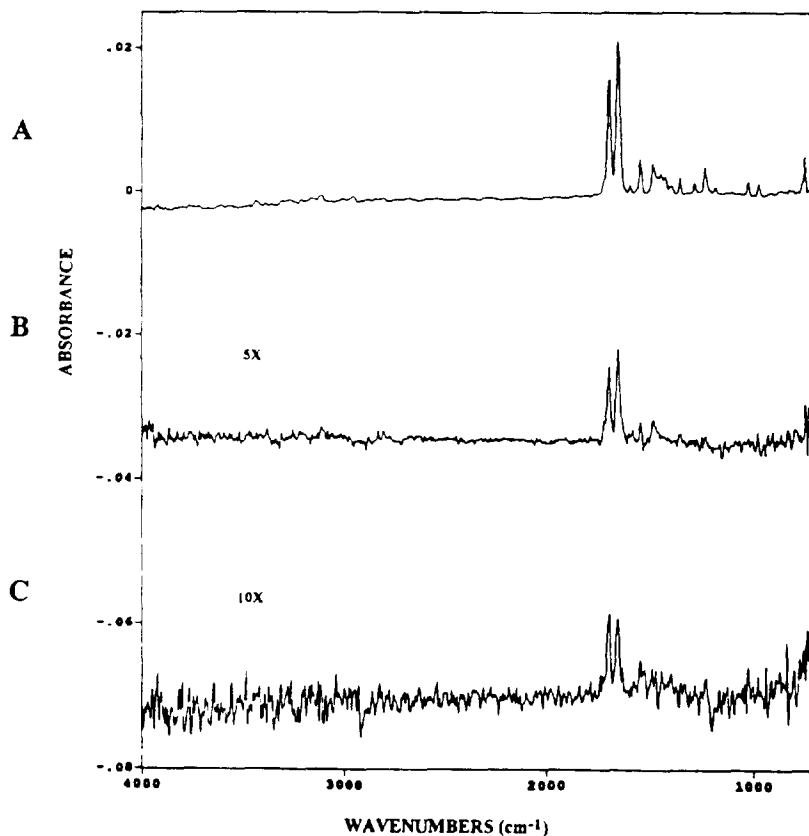


Fig. 6. DD SFC-FTIR spectra of caffeine from injections of (A) 3 ng; (B) 600 pg; and (C) 300 pg.

linearity of the concentration curves. The absorbance spectra obtained by averaging all of the spectra collected between the half-height points of each chromatographic peak were saved. The spectra were truncated and only the carbonyl region was curve-fitted by the LabCalc program. For acenaphthenequinone, only the strongest carbonyl band (approximately 1720 cm^{-1}) was investigated in these calculations. For caffeine, both strong carbonyl bands (approximately 1660 and 1700 cm^{-1}) were investigated.

The results for the 1720-cm^{-1} band of acenaphthenequinone were very similar to the func-

tional group chromatographic data. A correlation coefficient of 0.9996 was obtained for both spectral band area (from 600 pg to 60 ng) and height (300 pg to 60 ng). On the other hand, the results for the two carbonyl stretching bands of caffeine were surprising. The 1700-cm^{-1} band showed linear behavior over a fairly large range, whereas the 1660-cm^{-1} band did not. For the 1700-cm^{-1} band, the correlation coefficient for injected quantities between 300 pg and 120 ng was 0.9996 for area and 0.9995 for height (although the range had to be reduced to 600 pg–90 ng). The 1660-cm^{-1} band only showed linearity

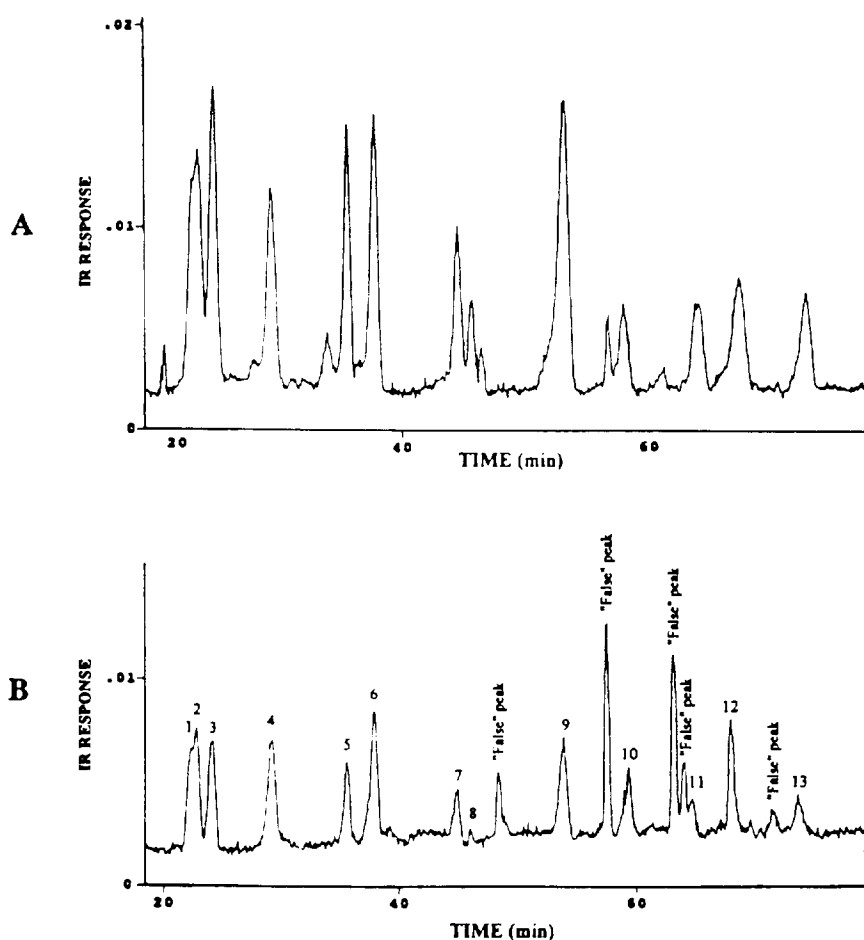


Fig. 7. Gram-Schmidt reconstructed chromatogram of the PAH mixture: (A) 20 ng of each component and (B) 5 ng of each component.

over short ranges of injected quantities. The behavior for the 1700-cm^{-1} and 1660-cm^{-1} bands can be readily seen in Fig. 5A and 5B, respectively. The plot for the 1700-cm^{-1} band shows only three points outside the control lines of $\pm 10\%$, but the plot for the 1660-cm^{-1} band shows only a few points *inside* these control lines. Similar results are seen for the corresponding plots using the peak height of the absorption bands, although the results using the height of the 1700-cm^{-1} band were not quite as good as the corresponding results using band area. One possible reason why the 1660-cm^{-1} band did not give rise to linear behavior could be because of absorption in this spectral region by ice on the ZnSe window. However, examination of the

spectra of acenaphthenequinone deposited in the same way did not show absorption due to ice near 1640 cm^{-1} , nor was there evidence of ice in the O–H stretching region of the caffeine spectra.

3.3. Identification

Identification of the separated components is often the ultimate goal in a chromatographic analysis. Identification can be accomplished with this interface by spectral searching the DD SFC–FTIR spectra obtained against a suitable database. Spectra from injections of caffeine of 3 ng, 600 pg and 300 pg are shown in Fig. 6. The

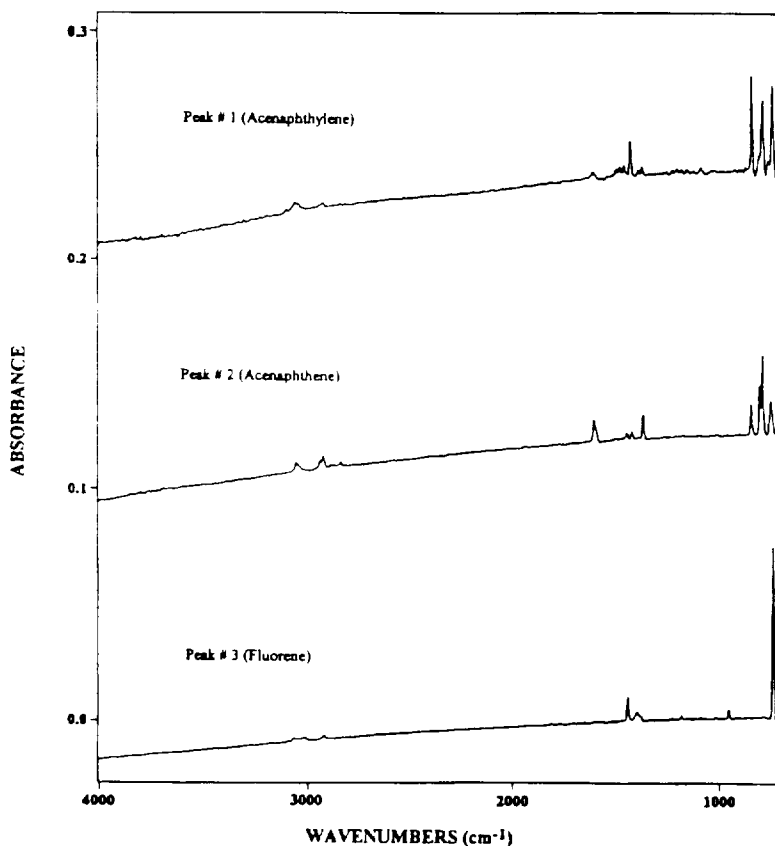


Fig. 8. IR Spectra of first three peaks of the DD SFC–FTIR data of an injection of the PAH mixture at a level of 5 ng per component.

minimum identifiable quantity, i.e., the amount needed to give a high enough S/N that spectral library searching routines can identify the compound, is about 600 pg for strong absorbers such as caffeine. Also shown in this figure is the spectrum of a 3-ng injection of caffeine where the S/N is sufficiently high for the spectrum to be considered to be of reference quality.

To test the sensitivity of the system using weakly absorbing analytes, real-time chromato-

grams of mixtures of polycyclic aromatic hydrocarbons (PAHs) (Supelprime-HC PAH mix, Supelco, Bellefonte, PA, USA), injected at levels of 20 and 5 ng per component were obtained. These compounds are notoriously weak infrared absorbers. The GS reconstructed chromatograms measured when each component was injected at a level of 20 and 5 ng are shown in Fig. 7. The spectra of the first three compounds to elute from the 5-ng injection are

Table 2

Comparison of the wavenumbers of the five highest intensity bands of the DD SFC-FTIR spectra of PAHs to the corresponding bands^a from the reference spectra in the Aldrich Library

Compound	No. 1	No. 2	No. 3	No. 4	No. 5
Peak ^b	ˆ783	1389	ˆ960	1593	1007
Naphthalene	ˆ780	^d	ˆ960	1595	1010
Peak No. 1	ˆ829	ˆ729	ˆ775	1427	1084
Acenaphthylene	ˆ830	ˆ725	ˆ775	1430	1080
Peak No. 2	ˆ783	ˆ799	ˆ841	ˆ737	1369
Acenaphthene	ˆ775	^e	ˆ835	ˆ745	1365
1590					
Peak No. 3	ˆ737	1447	1400	ˆ953	1188
Fluorene	ˆ740	1450	1410	ˆ955	1190
Peak No. 4	ˆ270	ˆ818	ˆ883	ˆ957	1242
Anthracene			ˆ880	ˆ950	
Phenanthrene	ˆ730	ˆ820			1250
Peak No. 5	ˆ775	ˆ748	ˆ825	1440	1134
Fluoranthene	ˆ775	ˆ745	ˆ825	1440	1135
Peak No. 6	ˆ837	ˆ748	1184	1597	961
Pyrene	ˆ840	ˆ750	1190	1590	965
Peak No. 7	ˆ744	ˆ883	ˆ814	895	949
Benz[<i>a</i>]anthracene	ˆ745	ˆ885	ˆ810	900	950
Peak No. 8	ˆ756	ˆ814	1261	1435	864
Chrysene	ˆ775	ˆ815	1265	^a	860
Peak No. 9	ˆ739	ˆ777	ˆ823	ˆ961	1437
No Aldrich reference of benzo[<i>a</i>]- or benzo[<i>k</i>]fluoranthene available					
Peak No. 10	ˆ756	ˆ825	ˆ837	ˆ849	ˆ880
Benzo[<i>a</i>]pyrene	ˆ760	ˆ820	ˆ835	ˆ850	ˆ875
Peak No. 11	ˆ810	ˆ741	ˆ887	1223	945
Dibenzo[<i>a,h</i>]anthracene	ˆ815	ˆ740	ˆ885	1220	945
Peak No. 12	ˆ729	837	1447	883	806
Indeno[1,2,3- <i>cd</i>]pyrene	ˆ730	835	^d	885	806
Peak No. 13	ˆ845	ˆ814	ˆ752	ˆ768	1145
Benzo[<i>ghi</i>]perylene	ˆ840	ˆ810	ˆ750	ˆ765	1145

^a Aldrich Library spectra rounded to the nearest 5 cm⁻¹.

^b Peak not shown in chromatograms shown in Fig. 7; this peak was visible in a few of the chromatographic runs.

^c Main band(s) in the spectra.

^d No corresponding band is seen in the reference spectra due to interference from the Nujol mull.

^e This band is an unresolved shoulder in the reference spectra.

^f Distinctive triplet in spectrum.

shown in Fig. 8. The S/N of the spectra shown is high enough to suggest that lower amounts than 5 ng of these compounds should be able to be detected; however, there are so few absorption bands in their spectra, and they absorb so close to the detector cut-off, that detecting the chromatographic peak caused by each eluted compound by the GS algorithm and, therefore, locating the deposited spots would be very difficult at injected levels much lower than 5 ng.

The identification of these compounds can be accomplished by comparison of the spectra with spectra from the Aldrich Library of Infrared

Spectra. A list of the five strongest absorption bands in the spectra from each of the chromatographic peaks and the five corresponding absorption bands of the spectra of the identified standards from the Aldrich library is shown in Table 2. Naphthalene is too volatile to be trapped in all of the chromatographic runs, as the temperature of the ZnSe window was not carefully controlled, but from one 20-ng injection and one 50-ng injection, a peak corresponding to naphthalene was observed at a retention time of about 17 min. The data for the naphthalene bands shown in Table 2 were obtained from a different 20-ng

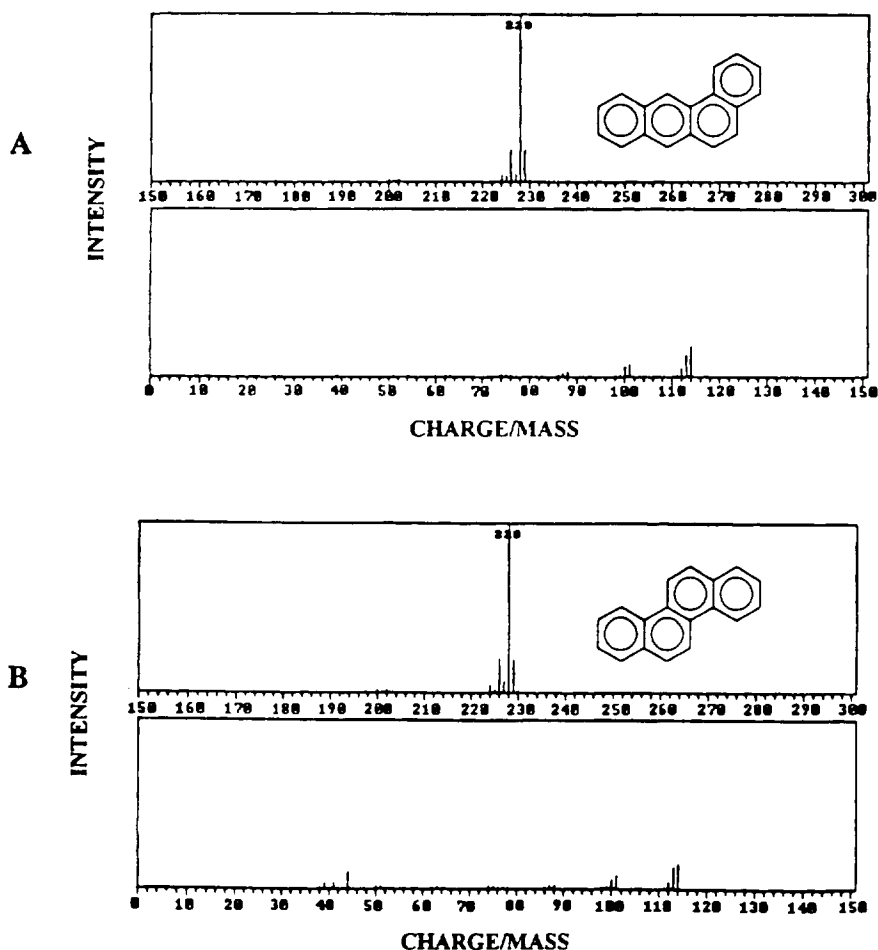


Fig. 9. Mass spectra from NIST/EPA/MSDC mass spectra database and structures of (A) benz[a]anthracene and (B) chrysene.

injection than the one shown in Fig. 7. Peak number 4 is caused by the coelution of anthracene and phenanthrene. The only spectrum not identified is from peak number 9, which is assumed to be from the unresolved elution of benzo[*b*]fluoranthene and benzo[*k*]fluoranthene. These isomers have similar structures and, therefore, would be expected to be very hard to separate. Neither of the compounds have reference spectra in the Aldrich library.

The infrared spectra give invaluable information for identification of PAHs as the mass spectra of PAH isomers are usually very similar. For example, the structures and mass spectra of chrysene and benz[*a*]anthracene (two C₁₈H₁₂ isomers) from the NIST/EPA/MSDC Mass Spectra Database are shown in Fig. 9. The mass

spectra of these two isomers are essentially identical, making identification by SFC–mass spectrometry very difficult. The infrared spectra of benz[*a*]anthracene and chrysene from an injection of 5 ng of each component are shown in Fig. 10. These spectra are very different and identification is easily accomplished by comparison to reference spectra.

3.4. 'False' peaks

Also seen in the GS reconstructed chromatograms shown in Fig. 7 are peaks labeled 'false' peaks. These type of peaks are occasionally seen in these chromatograms, but are easily distinguished from the true chromatographic peaks by examination of the spectra. Fig. 11 shows spectra

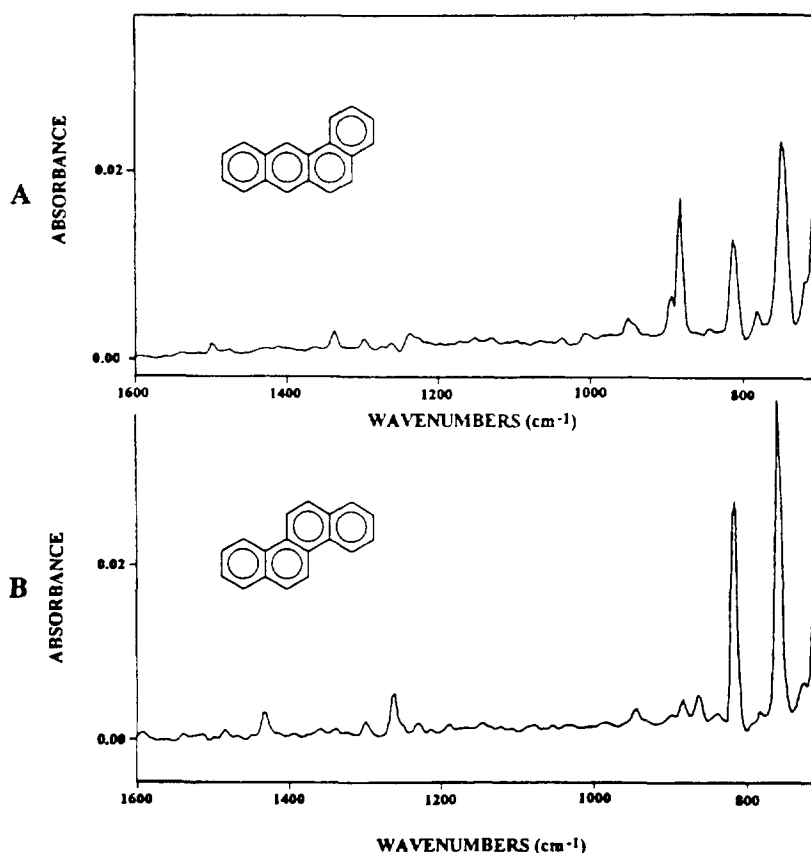


Fig. 10. DD SFC–FTIR spectra of 5 ng injection and structures of (A) benz[*a*]anthracene and (B) chrysene.

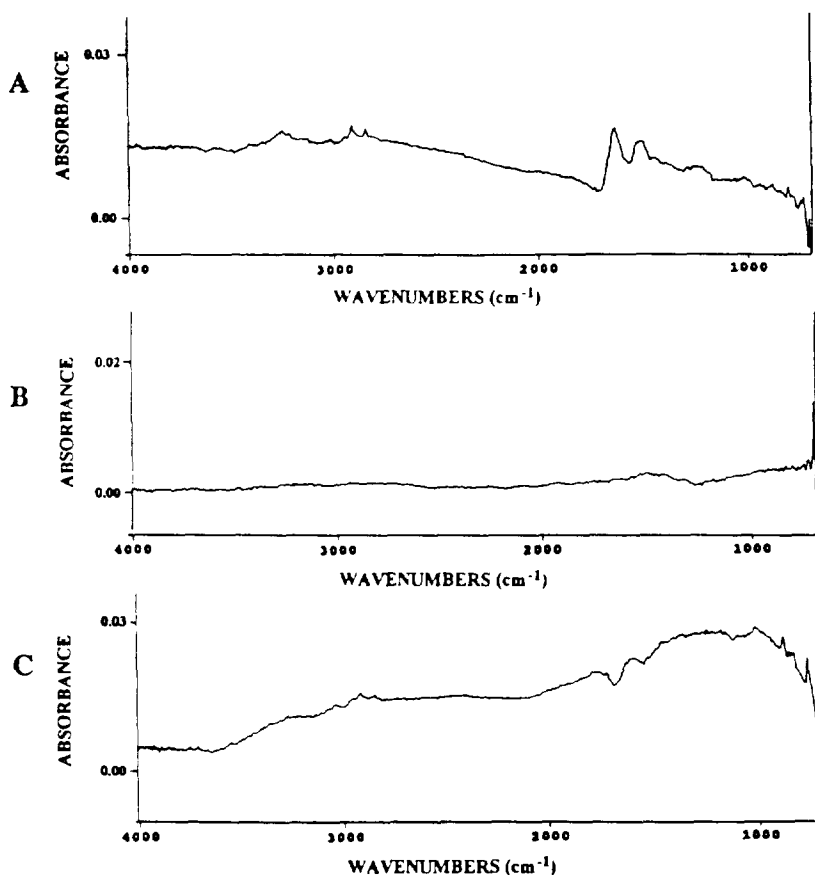


Fig. 11. IR spectra of 'false' peaks detected in the Gram-Schmidt reconstructed chromatograms of the PAH mixture: (A) spectrum of protein contaminant; (B) spectrum showing baseline shift; and (C) spectrum showing scattering effect from contaminant on window.

obtained from three false peaks in GS reconstructed chromatograms during the course of this investigation. The exact origin of each of these peaks is unknown, but probably arise from contaminants on the ZnSe window either absorbing some wavelengths or scattering the radiation, giving rise to a baseline shift. The spectrum in Fig. 11A appears to be a spectrum of a protein and may be attributable to a microscopically small piece of dead skin or dandruff. The spectrum in Fig. 11C appears to be represent the case where a baseline shift manifests itself as a chromatographic peak, or a combination of baseline shift from scattering and absorption by a protein contaminant. The spectrum shown in Fig. 11B is

of the false peak between peaks 12 and 13 of the chromatogram shown in Fig. 7B; this 'peak' appears to be solely caused by a baseline shift and should disappear if a chromatogram reconstruction algorithm that is insensitive to baseline variation been applied.

When FG chromatograms are obtained, no false peaks caused by baseline variations are usually observed. Fig. 12A shows a GS reconstructed chromatogram of 20 ng injected of the PAH mixture and Fig. 12B shows a chromatogram of the same injection computed by integrating the absorbance between 900 and 750 cm^{-1} . As seen from this figure, the false peaks of the GS chromatograms are not observed in the

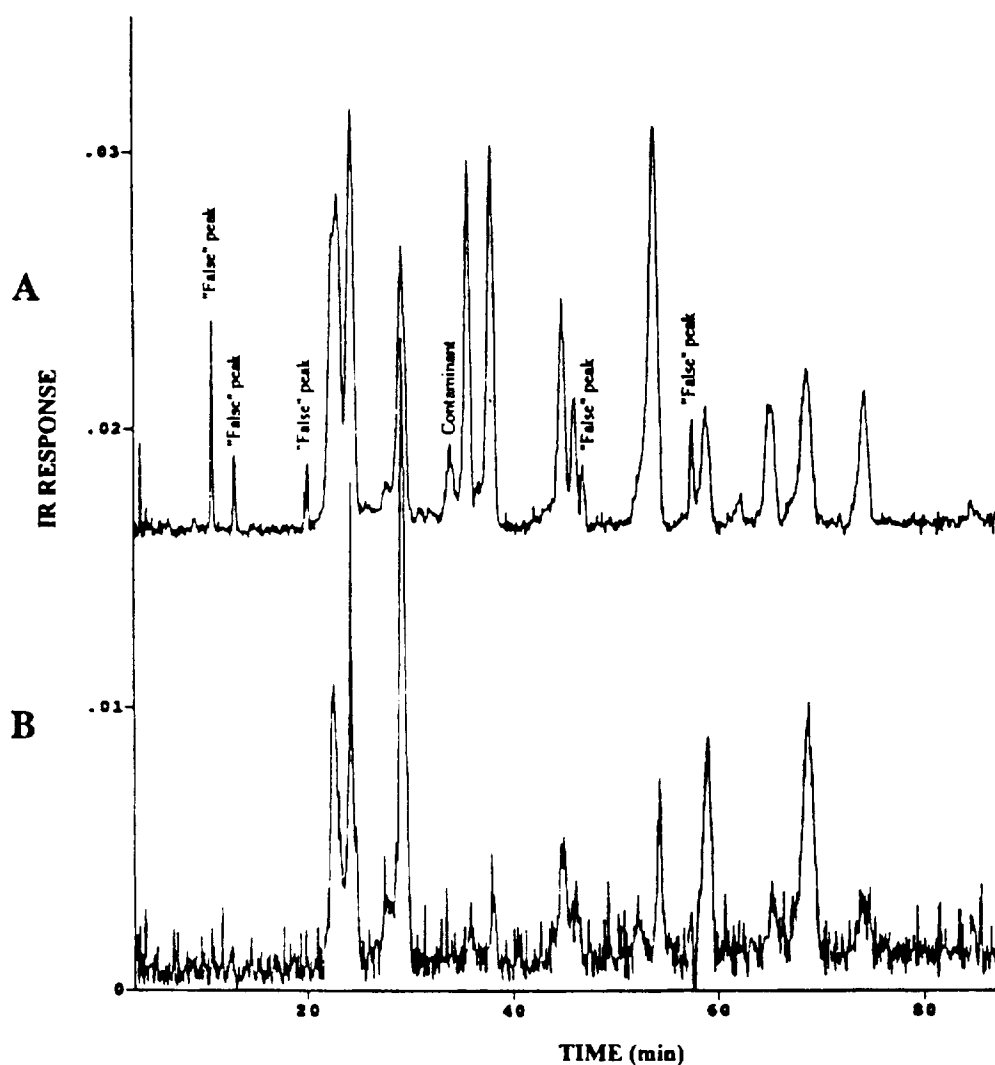


Fig. 12. Chromatograms of PAH mixture from the injection of 20 ng of each component: (A) Gram-Schmidt reconstructed chromatogram and (B) functional group chromatogram.

FG chromatograms, but the S/N is significantly worse, to the point that some real peaks are lost in the noise.

The S/N of FG chromatograms is usually greater than that of the corresponding GS chromatogram provided that the absorptivity of the analytical band(s) is large. The vibrational mode giving rise to the absorptions of PAHs in the region between 900 and 750 cm^{-1} is the C–H out-of-plane deformation, which is usually re-

garded as a strong band. Thus one might expect the S/N of the FG chromatogram (Fig. 12B) to be higher than that of the GS chromatogram (Fig. 12A). The probable reason why this is not the case is because the low wavenumber end of this region is very close to the detector cut-off, and the baseline stability of FTIR spectrometers usually degrades near the detector cut-off. Thus we believe that the low S/N of the FG chromatogram is more likely to have been caused by

Table 3
Elution order, names and structures of seven triazine herbicides

Elution order	Name	Structure
1	Prometon	
2	Propazine	
3	Atrazine	
4	Prometryne	
5	Simezine	
6	Ametryne	
7	Simetryne	

spectroscopic baseline instability than detector noise.

3.5. Addition of polar modifiers

The capability of adding polar modifiers to the CO₂ mobile phase and still obtaining useful DD SFC–FTIR data was then evaluated. A mixture of seven triazine herbicides, the elution order, names and structures of which are shown in Table 3, was injected into the system. The separation of these compounds is shown in the

chromatograms displayed in Fig. 13. The upper chromatogram shows the FID trace from the injection of 60 ng of each of the seven triazines separated with CO₂ as the mobile phase. The bottom two chromatograms are the GS reconstructed chromatograms from the FTIR data, with the middle trace being the separation of an injection of 10 ng each of the compounds using unmodified CO₂, and the bottom trace being the separation an injection of 6 ng of each of the compounds performed with CO₂ with 2% methanol as the mobile phase. No bands due to methanol were observed in any of the measured spectra. The first compound eluted, Prometon, is not seen in either of the chromatograms shown from the FTIR response. This peak was observed when the mixture containing 30 ng each of the compounds was injected into the system. The infrared response from Prometon in the 30 ng injection was approximately one-half of the response for the last two eluting peaks in the 30 ng injection, so it should have been observed in the 10 ng injection (Fig. 13B). The reason this compound did not adhere to the ZnSe window is unexplained, but Prometon is the only ether in the triazine mixture; the other triazines have a thioether group or a chlorine at the 1-position. Prometon is therefore slightly more volatile than the rest of the triazines and appears to evaporate completely when deposition at low injected quantities under these conditions. No effort was made to control the temperature of the window to better than ±10°C. Thus it is also possible that the window temperature was lower for the run when the Prometon peak was observed than when it was missing. If relatively volatile compounds are to be analyzed, the temperature of the plate can easily be lowered by 50°C by adding more dry ice to the methanol–dry ice mixture, but exact control of the temperature with this setup is not possible.

The peaks in the reconstructed chromatograms shown in Figs. 13B and 13C appear to tail more than the corresponding peaks measured in the absence of a polar modifier (Fig. 1A). There is no reason to suspect that the tailing occurs after the analytes have been deposited on the ZnSe substrate as the methanol co-solvent evaporates

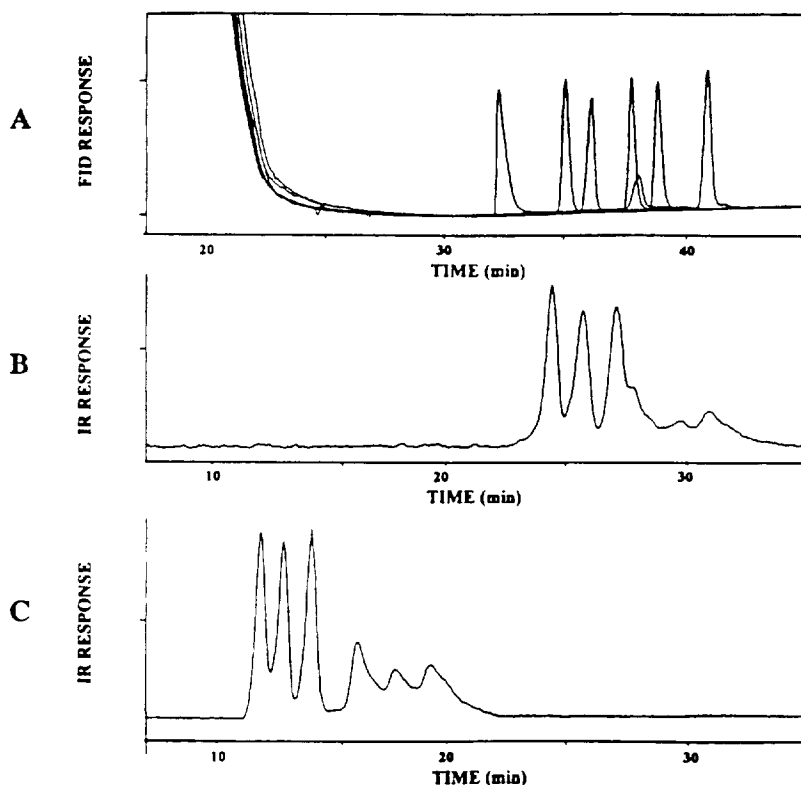


Fig. 13. Chromatograms of seven triazine herbicides: (A) FID traces for 60 ng of the components injected separately; (B) Gram-Schmidt reconstructed chromatograms of 10 ng injection separated with 100% CO₂; and (C) Gram-Schmidt reconstructed chromatogram of 6 ng injection separated with CO₂ containing 2% methanol.

along with the CO₂ immediately on leaving the restrictor. We can, therefore, only surmise that the presence of methanol in the mobile phase causes tailing of these analytes while they are eluting through the column.

4. Summary

We have demonstrated that the DD method for SFC-FTIR can be used for determining the amount of sample injected within approximately 10% by comparison to calibration curves from a standard. It is possible to get identifiable spectra from injections as low as 600 pg for strong infrared absorbers and between 1 and 10 ng for weak infrared absorbers. Finally, this interface allows for usage of polar modifiers in the mobile phase.

Acknowledgement

This work was supported in part by Cooperative Agreement No. CR-819576 with the U.S. Environmental Protection Agency.

References

- [1] K.H. Shafer, Pentoney and P.R. Griffiths, *Anal. Chem.*, 58 (1986) 58.
- [2] S.L. Pentoney, K.H. Shafer, and P.R. Griffiths, *J. Chromatogr. Sci.*, 24 (1986) 231.
- [3] S.L. Pentoney, K.H. Shafer, P.R. Griffiths and R. Fuoco, *J. High Resolut. Chromatogr. Chromatogr. Commun.*, 9 (1986) 168.
- [4] P.R. Griffiths, S.L. Pentoney, G.L. Pariente, and K.L. Norton, *Mikrochim. Acta Wien*; Vol. III (1988) 47.
- [5] M.W. Raynor, I.L. Davies, K.D. Bartle, A.A. Clifford, A. Williams, J.M. Chalmers and B.W. Cook, *J. High*

- Resolut. Chromatogr. Chromatogr. Commun.*, 11 (1988) 766.
- [6] M.W. Raynor, K.D. Bartle, I.L. Davies, A. Williams, A.A. Clifford, J.M. Chalmers and B.W. Cook, *Anal. Chem.*, 60 (1988) 427.
- [7] K.D. Bartle, M.W. Raynor, A.A. Clifford, I.L. Davies, J.D. Kithingi, G.F. Shilstone, J.M. Chalmers and B.W. Cook, *J. Chromatogr. Sci.*, 27 (1989) 283.
- [8] P.R. Griffiths, K.L. Norton and A.S. Bonanno, in K. Jinno (Editor), *Hyphenated Techniques in Supercritical Fluid Chromatography and Extraction*, Elsevier, Amsterdam, 1992, Ch. 7.
- [9] D.F. Gurka, S. Pyle, R. Titus and E. Shafter, *Anal. Chem.*, 66 (1994) 2521.
- [10] K.H. Shafer and P.R. Griffiths, *Anal. Chem.*, 55 (1983) 1939.
- [11] S.B. French and M. Novotny, *Anal. Chem.*, 58 (1986) 164.
- [12] M.E. Hughes and J.L. Fasching, *J. Chromatogr. Sci.*, 60 (1985) 2422.
- [13] J.W. Jordan, C.C. Johnson and L.T. Taylor, *J. Chromatogr. Sci.*, 23 (1986) 82.
- [14] M.W. Raynor, A.A. Clifford, K.D. Bartle, C. Reyne, A. Williams and B.W. Cook, *J. Microcol. Sep.*, 1 (1989) 101.
- [15] L.T. Taylor, in K. Jinno (Editor), *Hyphenated Techniques in Supercritical Fluid Chromatography and Extraction*, Elsevier, Amsterdam, 1992, Ch. 6.
- [16] M.W. Raynor, G.F. Shilstone, K.D. Bartle, A.A. Clifford, M. Cleary, and B.W. Cook, *J. High Resolut. Chromatogr. Chromatogr. Commun.*, 12 (1989) 300.
- [17] M.W. Raynor, G.F. Shilstone, A.A. Clifford and K.D. Bartle, *Microcol. Sep.*, 3 (1991) 337.
- [18] T.J. Jenkins, G. Davidson, M.A. Healy and M. Poliakoff, *J. High Resolut. Chromatogr.*, 15 (1992) 819.
- [19] P. Morin, B. Beccard, B., M. Caude and R. Rosset, *J. High Resolut. Chromatogr. Chromatogr. Commun.*, 11 (1988) 697.
- [20] K.H. Shafer, P.R. Griffiths and R. Fuoco, *J. High Resolut. Chromatogr. Chromatogr. Commun.*, 9 (1986) 124.
- [21] R. Fuoco, K.H. Shafer, and P.R. Griffiths, *Anal. Chem.*, 58 (1986) 3249.
- [22] K. Jinno and C. Fujimoto, *J. High Resolut. Chromatogr. Chromatogr. Commun.*, 4 (1981) 532.
- [23] K. Jinno, C. Fujimoto and D. Ishii, *J. Chromatogr.*, 239 (1982) 625.
- [24] K. Jinno, C. Fujimoto, and Y. Hirata, *Appl. Spectrosc.*, 36 (1983) 67.
- [25] K. Jinno, C. Fujimoto, and Y. Hirata, *J. Chromatogr.*, 258 (1983) 81.
- [26] C. Fujimoto, C., T. Osuka, and K. Jinno, *Anal. Chim. Acta*, 178 (1985) 159.
- [27] J.J. Gagel and K. Biemann, *Anal. Chem.*, 58 (1986) 2184.
- [28] J.J. Gagel and K. Biemann, *Anal. Chem.*, 59 (1987) 1266.
- [29] R.M. Robertson, J.A. de Haseth, J.D. Kiek and R.F. Browner, *Appl. Spectrosc.*, 42 (1988) 1365.
- [30] R.M. Robertson, J.A. de Haseth and R.F. Browner, *Appl. Spectrosc.*, 44 (1990) 8.
- [31] A.J. Lange, P.R. Griffiths and D.J.J. Fraser, *Anal. Chem.*, 63 (1991) 782.
- [32] A.M. Haefner, K.L. Norton, P.R. Griffiths, S. Bourne and R. Curbelo, *Anal. Chem.*, 60 (1988) 2441.
- [33] S. Bourne, A.M. Haefner, K.L. Norton and P.R. Griffiths, *Anal. Chem.*, 62 (1990) 2448.
- [34] T. Visser and M.J. Vredendregt, *Vibrational Spectrosc.*, 1 (1990) 205.
- [35] N.R. Smyrl, D.M. Hembree, Jr., W.E. Davis, D.M. Williams and J.C. Vance, *Appl. Spectrosc.*, 46 (1992) 277.
- [36] T. Visser, M.J. Vredendregt, A.P.J.M. de Jong, L.A. van Ginkel, H.J. van Rossum and R.W. Stephany, *Anal. Chim. Acta*, 275 (1993) 205.
- [37] D.M. Hembree, Jr., N.R. Smyrl, W.E. Davis and D.M. Williams, *Analyst*, 118 (1993) 249.
- [38] P. Jackson, G. Dent, D. Carter, D.J. Schofield, J.M. Chalmers, T. Visser and M. Vredendregt, *J. High Res. Chromatogr.*, 16 (1993) 515.
- [39] T. Visser, M.J. Vredendregt, A.P.J.M. de Jong, H.J. van Rossum, R.W. Stephany and L.A. van Ginkel *Analyst*, 119 (1994) 2681.
- [40] A.M. Haefner, K.L. Norton, H. Makishima and P.R. Griffiths, *The Pittsburgh Conference on Analytical Chemistry and Applied Spectroscopy, Atlanta, March 1989*, Paper 459.
- [41] K.L. Norton, A.M. Haefner, H. Makishima, G. Jalsoszky and P.R. Griffiths, *Appl. Spectrosc.*, (1995) submitted.
- [42] E.J. Guthrie and H.E. Schwartz, *J. Chromatogr. Sci.*, 24 (1986) 236.
- [43] J.A. de Haseth and T.L. Isenhour, *Anal. Chem.*, 49 (1977) 1977.
- [44] R. Cassidy and M. Janoski, *LC·GC*, 10 (1992) 692.